

Relaxation and coarsening of weakly-interacting breathers in a simplified DNLS chain

Stefano Iubini^{1,2}, Antonio Politi³, Paolo Politi^{4,2}

¹ Dipartimento di Fisica e Astronomia, Università di Firenze, via G. Sansone 1 I-50019, Sesto Fiorentino, Italy

² Istituto Nazionale di Fisica Nucleare, Sezione di Firenze, via G. Sansone 1 I-50019, Sesto Fiorentino, Italy

³ Institute for Complex Systems and Mathematical Biology & SUPA University of Aberdeen, Aberdeen AB24 3UE, United Kingdom

⁴ Istituto dei Sistemi Complessi, Consiglio Nazionale delle Ricerche, via Madonna del Piano 10, I-50019 Sesto Fiorentino, Italy

E-mail: stefano.iubini@unifi.it

Abstract. The Discrete NonLinear Schrödinger (DNLS) equation displays a parameter region characterized by the presence of localized excitations (breathers). While their formation is well understood and it is expected that the asymptotic configuration comprises a single breather on top of a background, it is not clear why the dynamics of a multi-breather configuration is essentially frozen. In order to investigate this question, we introduce simple stochastic models, characterized by suitable conservation laws. We focus on the role of the coupling strength between localized excitations and background. In the DNLS model, higher breathers interact more weakly, as a result of their faster rotation. In our stochastic models, the strength of the coupling is controlled directly by an amplitude-dependent parameter. In the case of a power-law decrease, the associated coarsening process undergoes a slowing down if the decay rate is larger than a critical value. In the case of an exponential decrease, a freezing effect is observed that is reminiscent of the scenario observed in the DNLS. This last regime arises spontaneously when direct energy diffusion between breathers and background is blocked below a certain threshold.

Keywords: Coarsening processes, Stochastic particle dynamics, Diffusion.

Submitted to: *Journal of Statistical Mechanics: theory and experiment*

1. Introduction

The one-dimensional Discrete NonLinear Schrödinger (DNLS) equation [1, 2]

$$i\dot{z}_n = -2|z_n|^2 z_n - \gamma(z_{n+1} + z_{n-1}) \quad (1)$$

with $1 \leq n \leq N$ and suitable boundary conditions describes the dynamics of a chain of interacting, anharmonic oscillators with complex amplitudes z_n . This equation was firstly derived in the 1950s by Holstein [3] within a tight-binding approximation for the motion of polarons in molecular crystals, but it can more generally be derived by a nonlinear Schrödinger equation with a simple cubic nonlinear term, once we discretize the Laplacian as a finite difference approximation. Since then, because of

its generality, it has become a prototypical model of wave propagation in nonlinear lattices [4] and provides a reasonably accurate description of several physical setups, ranging from trapped cold gases [5, 6, 7] to coupled optical waveguides [8, 9], from magnetic systems [10, 11, 12] to energy transport in biomolecules [13].

Upon identifying the set of canonical variables z_n and iz_n^* , Eq. (1) follows from the Hamilton equations $\dot{z}_n = -\partial H/\partial(iz_n^*)$ associated to the Hamiltonian

$$H = \sum_{n=1}^N \left[|z_n|^4 + \gamma(z_n^* z_{n+1} + z_n z_{n+1}^*) \right], \quad (2)$$

which is a conserved quantity along with the mass

$$A = \sum_n |z_n|^2. \quad (3)$$

The thermodynamical behavior of the DNLS equation depends on two main parameters: the energy density $u = H/N$ and the mass density $a = A/N$, which can be mapped unambiguously to a couple of values of temperature T and chemical potential μ . In the limit of a vanishing temperature, the lowest energy state can be determined by searching for a uniform state with constant amplitude $|z_n|$ and a constant phase shift between neighbouring sites, $z_{n+1} = z_n \exp(i\phi_0)$. Posing $z_n = |z| e^{i(n\phi_0 + \psi)}$, where ψ is an irrelevant n -independent quantity, it is found that $u = |z|^4 + 2\gamma|z|^2 \cos\phi_0$ and $a = |z|^2$. The minimization gives $\phi_0 = \pi$, so that the ground states lie along the line \mathcal{C}_0 , $u = a^2 - 2\gamma a$. States below \mathcal{C}_0 are not physically accessible. Moreover, by assuming $\psi = \omega_0 t$, it is found from Eq. (1) that a ground state rotates with a frequency $\omega_0 = 2(a - \gamma)$, which depends on its mass density.

In the limit of a diverging temperature, the coupling term on average vanishes as the phases are randomly distributed. Therefore, the mean frequency, $\omega = 2|z_n|^2$, is proportional to the local mass, which is distributed according to a Poisson distribution [14]. In fact, in the limit $\beta \rightarrow 0$ ($T \rightarrow \infty$) the statistical weight of a configuration, given by the grand canonical partition function, is proportional to $\exp(\eta A)$, where $\eta = \beta\mu$ is the (negative) finite limit of the product of the vanishing inverse temperature β by the diverging chemical potential μ . In conclusion, infinite-temperature states are characterized by an exponential distribution $P(|z_n|^2) = a^{-1} e^{-|z_n|^2/a}$, with $\langle |z_n|^2 \rangle = a$, so that they lie along the line \mathcal{C}_∞ , $u = \langle |z_n|^4 \rangle = 2a^2$.

Equilibrium states in between \mathcal{C}_0 and \mathcal{C}_∞ are *standard* positive-temperature thermodynamic states, while the points above \mathcal{C}_∞ belong to the so-called negative temperature region [14]. Although a grand canonical distribution is ill-defined for the negative-temperature DNLS [14, 15], negative temperature states can be consistently introduced within the microcanonical ensemble [15], where H and A are fixed quantities. The main feature of the negative temperature regime in the DNLS equation is the spontaneous appearance of localized excitations, called breathers [16], which collect the excess energy density ($u - 2a^2$). Since the local frequency of the phase of each oscillator is proportional to its mass, breathers are expected to rotate at a much larger frequency than other sites, usually named background. Direct microcanonical simulations of the DNLS chain show that, after some transient, the breather dynamics is essentially frozen for very long times [17], with a finite density of breathers which is constant in time and a negative microcanonical temperature. This is in contrast with analytical results based on entropic arguments [18, 19, 20, 21], whose conclusions lead to expect that the density of breathers should instead decrease in time and that the

expected final (equilibrium) state is made up of a single breather, which absorbs all the excess energy, surrounded by an infinite-temperature background.

A full understanding of this discrepancy in the deterministic DNLS model has not yet been reached, due to the difficulty of providing a consistent description of the interaction between a breather and the nearby fluctuating background over very long (i.e. thermodynamical) timescales. As a result, the problem of determining the macroscopic relaxation law that allows to reach the final single-breather state is still open. In order to gain insight into this problem, in this paper we study some simplified stochastic versions of the DNLS equation, as their dynamics can be much better controlled and characterized. These models have been selected so as to exhibit conservation laws, since we are convinced that these are key properties of the general scenario. A base version of the two main models was introduced in a previous publication [22]; it is here illustrated in Fig. 1, where we also stress the mutual relationships. The first model, panel (a), is obtained by neglecting the coupling term, i.e. by setting $\gamma = 0$ in the DNLS Hamiltonian. Since the critical line \mathcal{C}_∞ does not depend on the value of γ , we expect it to still hold in the stochastic model. In the limit of vanishing γ , the local phases of the DNLS oscillators do not play any role. Accordingly, it is convenient to introduce the local variable $a_n = |z_n|^2$ denoting the mass (or “height”) of the site n and the two conserved quantities (2) and (3) write as $H = \sum_n a_n^2$ and $A = \sum_n a_n$. The stochastic model dynamics is finally defined by introducing a local Microcanonical Monte Carlo (MMC) move. Given a randomly chosen triplet of consecutive sites, $(n-1, n, n+1)$, the local variables a_{n-1}, a_n, a_{n+1} are randomly updated under the only constraint of preserving the total energy and mass of the triplet. In the following we will refer to this model as the MMC model.

The second model, panel (b), can be considered as a further simplification of the DNLS dynamics and is better explained by distinguishing between breather and non-breather sites (also called background sites). The height is now an integer variable that we call c_n in order to mark the difference with respect to the previous setup. In the background c_n can only take the values 0 (empty site) or 1 (occupied site), while breathers are characterized by $c_n > 1$. The model is called partial exclusion process (PEP), because the space is divided into disjoint channels (the regions among breathers) where particles diffuse according to the exclusion constraint. Breather sites instead can freely emit and absorb particles towards/from the neighbouring background sites, until their height reduces to one, in which case they are absorbed by the background.

In both models, above the infinite temperature line, a slow dynamics manifests itself as a sort of coarsening of breather states, which has, however, no equivalent in the DNLS, where their dynamics essentially freezes. So, the question arises: what is the relevant ingredient which is missing in the stochastic models? An important, conceptual difference between the DNLS equation and the MMC/PEP models is the absence of a phase dynamics in the latter ones. In the original context, the local variable is indeed $z_n := \sqrt{a_n} e^{i\phi_n}$, while only a_n is present in the MMC. This is contrary to the approximation often invoked in the context of dissipative oscillators, where the amplitude dynamics is neglected, the phases being much more sensitive to the coupling strength [23]. The approach is, however, justifiable in our context when γ is small: in this limit, neither of the two conserved quantities depends on the phases, so that the physics is contained in the distribution of the amplitudes. Phases enter only in the coupling mechanism, which, in the MMC, has been designed just to capture entropic effects in the simplest possible way. As a result, one can

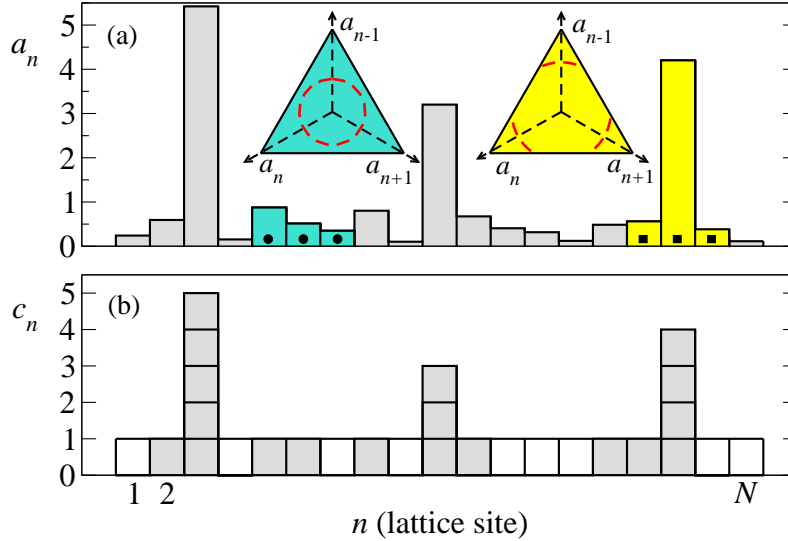


Figure 1. (a): The MMC model. A typical amplitude profile a_n displays a certain number of high-amplitude breathers superposed to a background. Left and right insets show in dashed red lines the available states respectively for a background triplet of sites (turquoise bars marked with black dots) and a triplet containing a breather (yellow bars marked with black squares). The legal configurations are obtained as intersection between a plane (main triangle) and a sphere (not shown) that account for local conservation of mass and energy, respectively. Due to the further constraint on the positivity of the amplitudes a_n , the allowed states may lie on three disconnected arcs, see the right inset. This happens when one of the three amplitudes is significantly larger than the others. (b): The PEP model. The amplitude profile in panel (a) is reproduced in terms of the integer amplitude c_n . White and grey squares highlight respectively empty ($c_n = 0$) and occupied ($c_n > 0$) sites.

claim that the disagreement between the coarsening dynamics (exhibited by MMC and PEP) and the evolution of breathers in the DNLS can be traced back to the way breather-background interaction is accounted for. More specifically, in the original DNLS, breathers of increasing amplitude rotate faster and faster (the frequency ω of a massive breather is equal to $2|z_n|^2 = 2a_n$). Therefore, the average coupling energy becomes increasingly weak upon increasing a_n . An explicit perturbative analysis of the DNLS is a subtle object that is currently under investigation. Here, we focus on simple stochastic models, where we have a full control of the evolution rule.

The weakening of the interaction induced by an increasingly fast rotation is here simulated by postulating that the coupling strength depends on the breather amplitude, which, from now on, is denoted with h . More precisely, we introduce the probability $\alpha \in (0, 1]$ for a move involving the breather to actually occur. After investigating the case of constant α (in order to test the correct scaling) we consider the more interesting case $\alpha = h^{-\beta}$. One of the major results of this paper concerns the coarsening exponent $1/\zeta$, defined from the time dependence of the average distance L between neighbouring breathers: $L(t) \sim t^{1/\zeta}$. We find

$$\zeta = \begin{cases} 3 & \beta \leq 1 \\ 2 + \beta & \beta > 1 \end{cases} . \quad (4)$$

Altogether, in section 2, we analyse the relaxation of a single breather for fixed small α in the PEP model, finding that the process is initially ballistic, and becomes diffusive at later times. A similar scenario is then found when α is assumed to depend on the breather height. In the following section 3, we focus on the interactions between neighbouring breathers, showing that the process is eventually diffusive. We also connect the value of the diffusion coefficient with the coarsening exponent. In section 4, we analyse more natural coupling schemes in the MMC, including one which leads to a logarithmically slow process, quite close to the scenario actually observed in the DNLS. Finally, in section 5, some conclusions are drawn and the open problems briefly summarized.

2. Relaxation of a single weakly-interacting breather

In this section we study the PEP model defined on a lattice of N sites with periodic boundary conditions, see Fig. 1(b). The variable c_n identifies the number of particles in the site n , which can be of background or breather type. In the former case, the particles diffuse as in a standard exclusion process, i.e. c_n can be at most equal to 1. The breathers are “reservoirs” ($c_n > 1$) which exchange particles with neighbouring (background) sites. If the breather content reduces to just a single particle (i.e., $c_n = 1$) it becomes a background site for ever. The evolution rule is simple: we randomly choose an ordered pair of neighbouring sites (i, j) , $j = i \pm 1$, and make the move $(c_i, c_j) \rightarrow (c_i - 1, c_j + 1)$ if and only if $c_i > 0$ and $c_j \neq 1$. This means that we move a particle if it exists and enters either an empty background ($c_j = 0$), or a breather site ($c_j > 1$). If the move involves a breather (i.e., either $c_i > 1$ or $c_j > 1$), it is accepted with probability α ; if it does not, it is always accepted.

At variance with both MMC and the original DNLS, in this model there is only one conserved quantity (the number of particles), accompanied by an additional constraint in the background, due to the exclusion rule. There is another difference between PEP and MMC/DNLS models: in the former one breathers do not arise spontaneously. In fact, according to above rules a breather can be destroyed but it cannot be created. This notwithstanding, the PEP model exhibits a slow dynamics (i.e. the coarsening of breathers) very similar to that of the MMC model, if the overall density of particles c is larger than $1/2$ [22]. In this respect, it is instructive to compare the critical density $c = 1/2$ of the PEP model with the infinite-temperature line $u = 2a^2$ of the MMC. For $T = \infty$, the MMC is characterized by a Poissonian distribution of masses, i.e. $\langle a^2 \rangle - \langle a \rangle^2 = \langle a \rangle^2$. In the PEP model, where a is a binary variable with average c , the above condition writes $c - c^2 = c^2$, whence $c = 1/2$.

In Fig. 2 we report the average evolution of a single breather of initial height $h(0) < N/2$ for different values of the coupling α . The breather is initially sitting on an empty background with periodic boundary conditions and the condition on $h(0)$ implies that the breather is eventually absorbed by the background \ddagger . In detail, we have chosen $h(0) = 100$, much smaller than $N = 10^4$, to reduce boundary effects during the breather relaxation. The results show the existence of two regimes separated by a crossover time $t_c \sim 1/\alpha^2$. For short times the average height of the breather decreases ballistically, $\langle \Delta h(t) \rangle \equiv \langle h(0) - h(t) \rangle \simeq \alpha t$, while for large times it decreases diffusively, $\langle \Delta h(t) \rangle \simeq \sqrt{t}$. At even longer times $\langle \Delta h(t) \rangle$ saturates because of the

\ddagger Indeed, the condition $h(0) < N/2$ corresponds to a global density $c < 1/2$, which can not sustain localized states when thermodynamical equilibrium is reached.

finite height of the breather, which runs out of particles. The different behavior at short/long times can be qualitatively understood as follows. At early times (especially if α is vanishingly small) released particles freely diffuse in a practically empty background with no mutual interaction and a vanishing probability to be reabsorbed. At long times, emitted particles have a much higher probability to return to the breather.

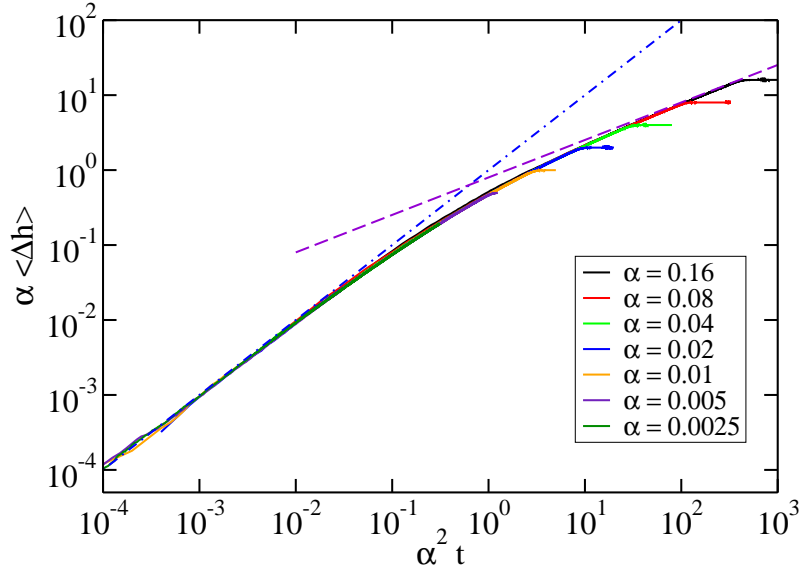


Figure 2. Evolution of the average height variation $\langle h(0) - h(t) \rangle$ of the breather during the relaxation process in rescaled units. Averages have been performed over 2000 different initial conditions. The dotted-dashed blue curve represents the analytical prediction for the ballistic growth, Eq. (12), and the dashed purple curve is the analytic prediction for the diffusive growth, see Eq. (13).

This argument can be made more rigorous under the approximation of continuous time and space variables. We proceed into two steps, by first deriving a set of mean-field differential equations for the probability $p_n(t)$ that the site n is occupied at time t (the breather being located in the site $n = 0$),

$$\begin{aligned} \dot{p}_n &\equiv \frac{\Delta p_n}{\Delta t} = \frac{1}{2} [p_{n-1}(1 - p_n) + p_{n+1}(1 - p_n) - p_n(1 - p_{n-1}) - p_n(1 - p_{n+1})] = \\ &= \frac{1}{2} (p_{n+1} + p_{n-1} - 2p_n) \quad n > 1 \end{aligned} \quad (5)$$

and

$$\begin{aligned} \dot{p}_1 &\equiv \frac{\Delta p_1}{\Delta t} = \frac{1}{2} [\alpha(1 - p_1) - \alpha p_1 + p_2(1 - p_1) - p_1(1 - p_2)] \\ &= \frac{1}{2} [\alpha(1 - 2p_1) + (p_2 - p_1)], \end{aligned} \quad (6)$$

where $\Delta t = 1$ corresponds to the implementation of N random moves (N is the lattice size). The evolution equation for p_1 can be made formally equivalent to the bulk dynamics (5) upon introducing a p_0 such that

$$\alpha(1 - 2p_1) + (p_2 - p_1) = (p_0 + p_2) - 2p_1. \quad (7)$$

As a next step, we introduce the continuous variable $x = n - 1$ and the corresponding probability density $\rho(x, t) = p_n - 1/2$, so that the stationary solution is $\rho(x) = 0$. Under the approximation of a weak dependence of ρ on the spatial variable x (which becomes increasingly correct at long times), the bulk dynamics is described by a standard diffusive equation

$$\partial_t \rho(x, t) = D \partial_{xx} \rho(x, t), \quad (8)$$

where $D = 1/2$. Moreover, one can assume[§] $p_0 = \rho(0) + 1/2 - \rho_x(0)$, so that Eq. (7) transforms into the boundary condition

$$\rho_x(0) = 2\alpha\rho(0) \equiv r\rho(0). \quad (9)$$

Therefore, we recover the well known result that the exclusion process is purely diffusive [24] and find that the interaction with the breather can be modelled by a Robin (semi-reflecting) boundary condition in $x = 0^+$, gauged by the variable r . For $\alpha \rightarrow \infty$, the Robin condition reduces to a standard absorbing boundary condition, $\rho(0) = 0$, while for $\alpha \rightarrow 0$, it corresponds to a reflecting boundary, $\rho_x(0) = 0$. The case $\alpha = 1$, studied in Ref. [22], corresponds to an intermediate setup, characterized by a finite interaction time-scale, because for $\alpha = 1$ attachment occurs on the time scale of diffusion.

We now want to determine the average height reduction $\langle \Delta h(t) \rangle$ of a breather due to the particles that have been emitted but *not yet* reabsorbed. To this end, we need to know the probability $F(t)dt$ that a particle is being reabsorbed in the time interval $(t, t + dt)$. This quantity can be evaluated exactly using the continuum model and assuming that a particle is released in $x = x_0$ at $t = 0$ and it is thereby let free to diffuse in $[0, \infty]$. Note that the value of x_0 is not crucial for the continuum model as long as it is chosen to be close to the origin. The analytical expression for $F(t)$ valid for all t is fairly complicated and it is given in Appendix A. Here we limit to give its expression for short and long times,

$$F(t) \simeq \begin{cases} 4\alpha\sqrt{D/(\pi t)} & x_0^2 \ll t \ll \alpha^{-2} \\ 1/(2\alpha\sqrt{\pi Dt^3}) & t \gg \alpha^{-2} \end{cases}. \quad (10)$$

The height reduction $\langle \Delta h(t) \rangle$ of the breather is thereby obtained by integrating over all particles that have been emitted and not yet absorbed at time t . However, we must be careful, because the evaluation of the number of emitted particles (either reabsorbed or not) is not trivial: the emission of a particle from the breather is possible only if the neighbouring site, which should receive it, is empty. Since the initial condition corresponds to an empty background, at short times the probability $(1 - p_1)$ that the neighboring sites are empty is practically equal to 1. On the other hand, at long times, after many emissions of particles, the region around the breather is almost at equilibrium, corresponding to $p_1 = 1/2$. In general, one can write

$$\langle \Delta h(t) \rangle = \alpha \int_0^t dt' (1 - p_1(t')) \int_{t'}^\infty dt'' F(t''). \quad (11)$$

Using the limiting expressions for $F(t)$ (provided in Eq. (10)) and for $p_1(t)$ (discussed here above), we find the following two regimes,

$$\langle \Delta h(t) \rangle \simeq \alpha t \quad x_0^2 \ll t \ll \alpha^{-2} \quad (12)$$

$$\langle \Delta h(t) \rangle \simeq \sqrt{\frac{2t}{\pi}} \quad t \gg \alpha^{-2}, \quad (13)$$

[§] Let us remind that $\rho(0) + \frac{1}{2}$ corresponds, in the discrete lattice, to p_1 .

where we have used $D = 1/2$. The details of the derivation of Eqs. (12) and (13) are given in Appendix B. These limiting behaviors are plotted in Fig. 2 and show a very good agreement with numerical simulations.

So far we have considered a constant coupling strength α . We now turn to a more physical case where α varies with the breather height

$$\alpha(h) = h^{-\beta}$$

and β is a real and positive parameter. The dependence of α on h is such that the higher a breather is, the lower is its coupling with the background. This also implies that the effective coupling is implicitly time-dependent. The data obtained for different β -values are reported in Fig. 3, using the same scaling ansatz as before, with the only difference that now, α is referred to the initial amplitude (i.e. $\tilde{\alpha} = \alpha(h(0))$).

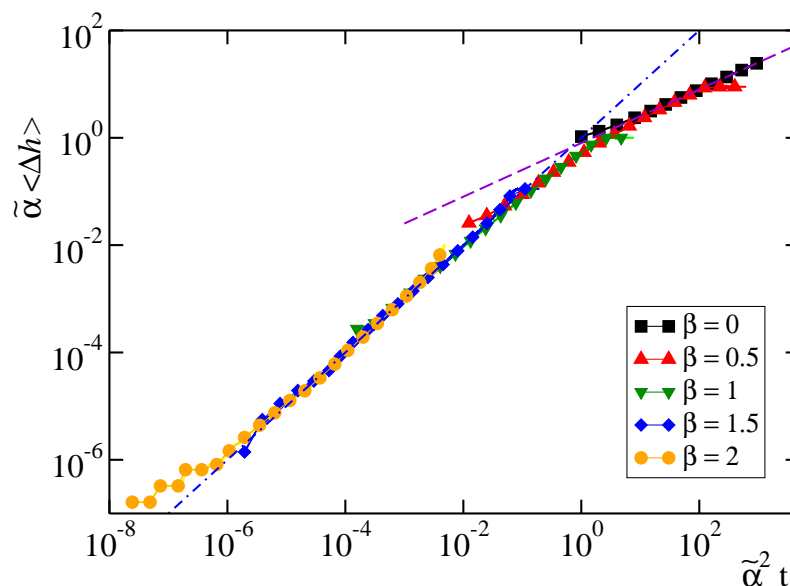


Figure 3. Breather relaxation dynamics for different choices of the coupling exponent β . Simulations refer to a setup with $N = 10000$ lattice sites and a breather with initial height $h(0) = 80$. The PEP channel is initially empty. Data are averaged over 1000 realizations. The dotted-dashed and dashed curves represent the analytical predictions as in Fig. 2, with α replaced by $\tilde{\alpha}$.

We interpret this result as an indication that even in the regime where α decreases with a power of h , the relaxation of the breather displays essentially the same behaviour of the case of α constant. The good data collapse obtained in Fig. 3 shows that the relevant timescale of the overall process is the slowest one, namely $\tilde{\alpha}^{-2}$.

3. Breather interactions

Here we are mostly interested in determining the exponent ζ which controls the way the density d_B of breathers decays in time ($d_B \approx t^{-1/\zeta}$). In order to do so, it is first necessary to understand how breathers interact with each other. After some transient, a set of breathers is present, which sit on a background characterized by

the occupation density $\rho = 1/2$. Let the origin of the time variable be set at such a stage, when the average distance between neighbouring breathers is L , while their average height is $\bar{h} = kL$, with $k > 0$ (this ensures that the surplus of energy contained in the breathers is an extensive quantity). In these conditions the background is “in equilibrium” at $T = \infty$ and, on average, the breathers do neither absorb nor release particles. However, the particles stochastically emitted can occasionally diffuse and be absorbed by a neighbouring breather. This mechanism couples breathers, which can exchange particles through the background, therefore inducing a diffusion of breathers’ height. Let us focus on a couple of breathers with initial height $h(0) = kL$. The square displacement σ^2

$$\sigma^2 \equiv \langle (h(t) - h(0))^2 \rangle \quad (14)$$

is expected to grow as $\sigma^2 = D_B t$, where $D_B(L)$ is the diffusion constant of the exchange process. By definition, one of the two breathers is completely absorbed after a time τ , when $\sigma^2(\tau) \simeq h^2(0)$. Therefore the absorption time τ scales with L as $\tau(L) \simeq h^2(0)/D_B(L)$. In order to determine the coarsening exponent it is necessary to invert the relation $d_B \approx \tau^{-1/\zeta}$, once set $d_B = 1/L$ and $h^2(0) \simeq L^2$. Accordingly,

$$L \simeq \left(\frac{L^2}{D_B} \right)^{1/\zeta}. \quad (15)$$

As a result, the coarsening exponent is fully determined by the scaling of D_B with L .

With reference to the two-breather setup, D_B can be expressed as the product of the rate γ to release a particle tout court by the probability P_c that the particle is absorbed by the neighboring breather (instead of being absorbed back by the emitter). An analytical calculation of P_c is reported in Appendix C for a simple geometry consisting of only two breathers placed at the boundaries of a PEP channel with fixed boundary conditions. For this setup,

$$\gamma = \frac{\alpha}{2}, \quad P_c(L, \alpha) = \frac{1}{2(1 + L\alpha)} \quad (16)$$

and therefore

$$D_B(L, \alpha) = \frac{\alpha}{4(1 + L\alpha)}. \quad (17)$$

When α scales with the breather height, i.e. when $\alpha = \bar{h}^{-\beta} = (kL)^{-\beta}$, the above equation provides the relevant scaling of D_B with the system size L . In particular, we find

$$D_B = \begin{cases} \frac{S(k, \beta, L)}{L} & \beta \leq 1 \\ \frac{S(k, \beta, L)}{L^\beta} & \beta > 1 \end{cases}, \quad (18)$$

where $S(k, \beta, L)$ is a prefactor weakly dependent on L for large L . Explicitly,

$$S(k, \beta, L) = \begin{cases} \frac{k^{-\beta} L^{1-\beta}}{4(1 + k^{-\beta} L^{1-\beta})} & \beta \leq 1 \\ \frac{k^{-\beta}}{4(1 + k^{-\beta} L^{1-\beta})} & \beta > 1 \end{cases} \quad (19)$$

Altogether, from Eq. (16) we finally obtain $\zeta = 3$ for $\beta \leq 1$ and $\zeta = (2 + \beta)$ for $\beta > 1$.

In Fig. 4 we show the growth of $\sigma^2(t)$ as obtained by directly simulating the evolution of a PEP model where two breathers are initially superposed to a background

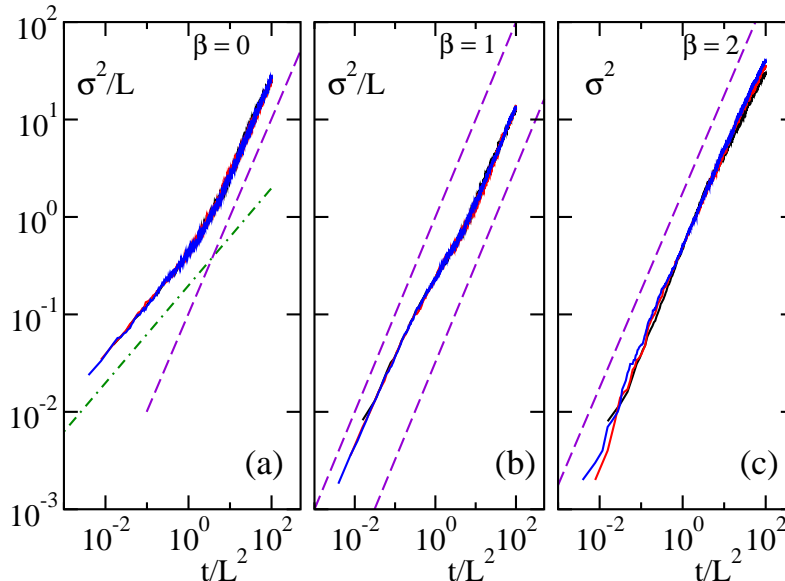


Figure 4. Evolution of the amplitude fluctuations σ^2 of two breathers sitting on an infinite temperature background for different coupling exponents β . Black, red, and blue full lines (indistinguishable) correspond to $N = 64$, 128, and 256, respectively. Data are obtained by averaging over a set of 1000 independent trajectories. The initial condition consists of two breathers of equal amplitude $h(0) = N = L$ at the boundaries of the chain. Dotted-dashed (green) and dashed (purple) lines correspond to a square root and linear increase of σ^2 , respectively.

in equilibrium at infinite temperature (i.e., with a density $1/2$). Horizontal and vertical axes are rescaled so as to collapse data corresponding to different system sizes on a single curve. In all cases, the growth of σ^2 is asymptotically linear: $\sigma^2(t) \sim t/L$ for $\beta = 0$ and $\beta = 1$, while $\sigma^2(t) \sim t/L^2$ for $\beta = 2$, in agreement with the prediction in Eq. (18). A detailed check of the prefactor $S(k, \beta, L)$ extracted from numerical simulations, is presented in Fig. 5, where it is compared with the analytical formula, Eq. (19). An excellent agreement is found.

It is interesting to notice that the asymptotic linear growth of σ^2 , which confirms the eventual diffusive behavior of the breather amplitude, may be preceded by a sub-diffusive behavior, where $\sigma \simeq t^{1/4}$ (see the green dotted curve in Fig. 4). This behavior can be understood by invoking a somehow unexpected relationship with surface roughening phenomena [24]. Consider a finite PEP extending from site 0, where it is in contact with a breather, to site L where fixed boundary conditions are imposed. Let $c_i(t)$ be a variable denoting whether a particle is present or not on site i at time t and introduce

$$C_j(t) = \sum_{i \geq j}^L c_i(t).$$

The variable $C_j(t)$ counts the number of particles present in the system on the right of the site j . It can be written as $C_j(t) = (L - j)/2 + s_j(t)$, where $s_j(t)$ can be interpreted as a rough interface of vanishing average height. Therefore the fluctuations of $s_0(t)$ (and thereby of $C_0(t)$), represent the fluctuations of the breather height as

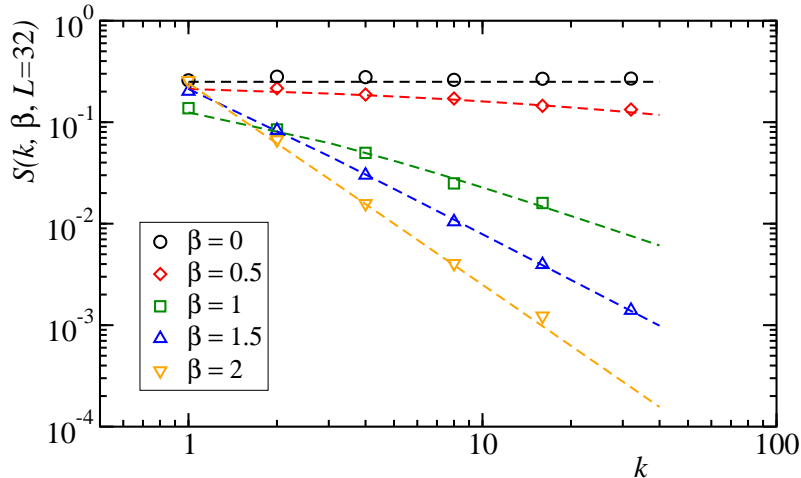


Figure 5. The diffusion prefactor $S(k, \beta, L = 32)$ (open symbols) computed from a fit of the asymptotic growth of $\sigma^2(t)$ for different values of β and k in a chain of $N = 32$ sites. Dashed lines are obtained from the analytical prediction in Eq. (19). Simulations are performed by superposing two breathers with amplitude $h(0) = kL$ at the two boundaries of a PEP chain at infinite temperature and with fixed boundary conditions. The breather interaction probability is $\alpha = h(0)^{-\beta}$. For each choice of k and β , the mean square height displacement σ^2 is computed by averaging over 1000 independent trajectories. The coefficient $S(k, \beta, L = 32)$ is therefore extracted by performing a linear fit of σ^2 in the asymptotic region where $\sigma^2 \sim t$.

well as the fluctuations of the rough surface. In the contexts analysed in this paper the bulk dynamics is fully linear, so that it is appropriate to invoke an analogy with the Edwards-Wilkinson model, whose fluctuations are precisely characterized by the exponent $1/4$ [25] seen in Fig. 4 for $\beta = 0$.

This “early time” behavior appears because in between the emission of a particle from a breather and the next emission, the system may not have the time to reach local equilibrium when β is small. $\beta = 1$ is the limiting value for the observation of the initial slow growth. In this critical case, the anomaly reduces to just a different multiplicative coefficient in front of the linear term, see Fig. 4(b).

We conclude this Section with the remark that above derivation of $\tau(L)$ applies to any $\alpha(L)$ dependence so long as it represents a coupling which weakens upon increasing the breather height. This includes an exponential dependence, in which case the time required for the death of a breather grows exponentially with its size.

4. The MMC model

Here, we discuss the coarsening process in the MMC setup. As briefly anticipated in the introduction, the evolution rule is a typical microcanonical Monte Carlo move restricted to neighbouring particles, so as to maintain the locality of the interactions of the DNLS equation. In practice, a triplet of neighbouring sites, $(n - 1, n, n + 1)$, is randomly chosen and the variables (a_{n-1}, a_n, a_{n+1}) updated so as to conserve mass and energy.

The positivity of a_n implies that when a high-mass (breather) site is involved

(see Fig. 1(a)), the accessible phase space reduces, to the point that, if a finite mass were concentrated in a single site, the two neighbouring ones being perfectly empty, no redistribution would be possible at all. In the absence of the condition for the mass to be positive, the rule would be equivalent to a stochastic scheme which preserves kinetic energy and linear momentum, of the type used to “ergodize” chains of oscillators [26, 27, 28, 29], where no such exotic phenomena are observed.

The same analysis carried out in the previous sections for the PEP, could be repeated for the MMC, by introducing a suitable height-dependent coupling. We have verified that this leads to the same scenario and, therefore, we do not see a compelling reason to show the corresponding results. We rather propose some considerations which make the weakening assumption less ad hoc than introducing a priori a dependence of the probability α on the breather height.

We start by quickly reminding that in the MMC model [22] we choose a random triplet of neighboring sites and update their amplitudes under the constraint of constant mass, $a_{n-1} + a_n + a_{n+1} = \bar{a}$, and constant energy, $a_{n-1}^2 + a_n^2 + a_{n+1}^2 = \bar{u}$. These two conditions correspond to the intersection of a sphere with a plane in the three dimensional phase space, a_{n-1}, a_n, a_{n+1} . Since a_n represent a mass it must be positive. This implies that the intersection is a full circle if the initial amplitudes are comparable, while it is made up of three, disconnected arcs if one of the sites has an initial amplitude significantly larger than the others (see Fig. 1(a)). In practice, this occurs when one of the three sites is occupied by a breather.

A first consequence of the results of the previous section is that different microscopic rules for the evolution of the system may produce the same coarsening exponent $1/\zeta$. More specifically, we remind that in Ref. [22] the MMC rule was implemented by restricting the random selection to the fully positive triplets, i.e. choosing points which lie inside the allowed arcs (this could be the entire circle). Here we consider a possible variation of the above dynamics that amounts to always selecting a point along the full circle and accepting the move only if the positivity condition is satisfied for the three amplitudes. Compared to the former recipe, which corresponds to $\alpha = 1$, i.e. $\beta = 0$, the latter algorithm avoids the identification of the arc extrema as functions of the mass and energy of the triplet. On the other hand, the dynamics is slowed down whenever the algorithm generates a triplet with at least one negative amplitude. Therefore one expects that this change of rule affects the probability α to effectively perturb a breather.

We now show that the slowing down corresponds to $\alpha \sim L^{-1/2}$, i.e. $\beta = 1/2$. Consider a triplet that contains one breather site with amplitude b and two background sites with amplitude xb and yb , with $x, y \ll 1$ and let ϵ denote the angular length of each arc^{||}. Then, the probability P_a that a randomly chosen move is acceptable is given by the ratio $3\epsilon/2\pi$, where the denominator is the amplitude of the set of moves that conserve mass and energy and the numerator accounts for the amplitude of the physical interval (i.e. the set of moves that satisfy also positivity). Since to leading order $\epsilon = \sqrt{3}(x+y)$ [22], ϵ scales as $1/b$ when the background amplitude is kept fixed and then also $P_a \sim 1/b$. Moreover, considering that the quantity diffusing during the MMC dynamics is the energy $u = b^2$ [22], $P_g \sim u^{-1/2}$, so that $\alpha \sim L^{-1/2}$. According to the discussion of previous Section, the difference between the two β exponents, $\beta = 0$ and $\beta = 1/2$, is not sufficient to induce a different coarsening law, which is

^{||} By symmetry reasons the three arcs have the same length ϵ . When ϵ equals $2\pi/3$, they merge into the entire circle.

again characterized by the exponent $\zeta = 1/3$ (data not shown).

Finally, we discuss a modification of the model which naturally leads to an exponentially slow dynamics, without the need to introduce explicitly an exponential decrease of α with L . In practice, we introduce a threshold Γ for the minimal arc angle to be considered. In other words, whenever the arc angle ϵ is smaller than Γ , no action is taken: the triplet configuration is left unchanged.

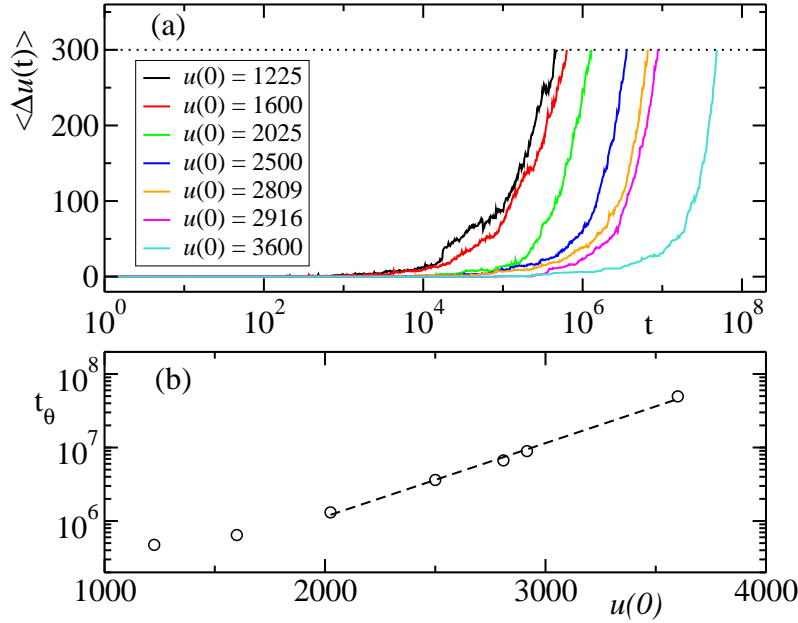


Figure 6. (a): Average energy reduction $\langle \Delta u(t) \rangle \equiv \langle u(0) - u(t) \rangle$ of one breather in a modified MMC model with interaction threshold $\Gamma = \pi/8$ for different initial energies $u(0)$. At $t = 0$ the breather is superposed to an MMC chain in equilibrium at temperature $T = 10$ with mass density $a = 1$ and $L = 2048$. The initial equilibrium distribution of the background is sampled by applying a Metropolis thermostat at $T = 10$ to each site of the chain for a transient $t_{th} = 5 \cdot 10^5$. $\langle \Delta u(t) \rangle$ is computed by averaging over 40 independent trajectories (up to the threshold $\theta = 300$). (b): Relaxation time (open circles) t_θ to reach the threshold as a function of the initial breather energy $u(0)$. The dashed line refers to an exponential fit $t_\theta \sim \exp(u(0)/E)$ with $E = 430$.

Once again, let us analyse the implications of the algorithm when the chosen triplet contains one breather and two background sites with amplitude b, xb, yb respectively. So long as both x and y are small the dynamics is blocked, since $\epsilon = \sqrt{3}(x + y) < \Gamma$. One may naively conclude that sufficiently high breathers are completely decoupled from the background. This is not true, because the background fluctuations can eventually lead to sufficiently large x or y values, so that the probability of such move is related to the probability of generating sufficiently large amplitudes in the neighbouring sites. More precisely, let us consider the grand canonical equilibrium distribution of the background amplitudes a_n reads

$$P(a_n) = \frac{1}{Z} \exp[-\beta(a_n^2 - \mu a_n)], \quad (20)$$

where $\beta = 1/T$ and μ are the inverse (positive) temperature and the chemical potential

of the background, while $Z = \int_0^\infty \exp[-\beta(a_n^2 - \mu a_n)] da_n$ is the partition function. The probability to have a mass fluctuation comparable to the breather height b (the square root of the energy) is exponentially small in b and depends on the values of β and μ . In fact, a direct simulation of the modified MMC model with $\Gamma = \pi/8$ (see Fig. 6(a)), shows that breathers well above the interaction threshold evolve according to an effective coupling exponentially small in the breather energy.

With reference to the parameters of Fig. 6, $\beta = 0.1$ and $\mu = -6.46$ ¶. In the range of chosen breather energies ($u(0) > 1000$), the term in μ in $P(a_n)$ can be neglected, so that the probability of the fluctuation is controlled by the local energy a_n^2 . This is confirmed in Fig. 6(b), where the relaxation time t_θ necessary to release an amount of energy θ from the breather to the background is shown to depend exponentially on the initial breather energy $u(0)$. Altogether, the above analysis shows that an exponentially small coupling between breathers and background may arise as a consequence of background fluctuations when energy diffusion is blocked by additional constraints. In this regime, the analysis of the previous section predicts a logarithmic coarsening of the breathers.

5. Conclusions

The deterministic DNLS equation and the stochastic MMC/PEP models have the common feature that their phase diagram includes a high-energy region where localized excitations can appear (DNLS and MMC) or can be preserved (PEP), at least. Breather dynamics is frozen in DNLS, while it is normally slowed down, but not frozen, in MMC/PEP. The slow dynamics in stochastic models corresponds to a coarsening process where breathers exchange mass until a breather loses so much mass that it is absorbed by the background, leading to a reduction of breather density.

This coarsening process follows a power-law and it is more or less slow, depending on the strength of the breather-background interaction. Our results support the idea that the extremely slow (almost frozen) dynamics observed in DNLS is due to the weakening of the interaction with breathers of increasing height. However, a power law weakening of the breather-background coupling maintains a power-law coarsening. For this reason, the results of section 4 are particularly instructive. There, we have studied a variant of the MMC model, where the breather-background interaction is regulated by a threshold rather than by a direct coupling: in fact, we impose there is a minimum transfer of mass. Upon increasing the breather height, this condition can be satisfied only if a neighbouring site is substantially higher than usual, an event that is exponentially rare and highly intermittent.

This mechanism, postulated a priori in the MMC model, might be active in the DNLS as a result of the combination of the usually very weak interaction of high-amplitude breathers (due to their fast rotation) with rare, relatively-strong, energy transfers due to occasional resonant interactions with neighbouring sites. A detailed investigation of this conjecture is in progress.

¶ The chemical potential μ has been determined by solving the equation $a = \int_0^\infty P(x)x dx$ with $\beta = 0.1$ and $a = 1$.

Appendix A. Diffusion with a single semi-reflecting boundary

We want to solve the diffusion equation,

$$\frac{\partial p}{\partial t} = D \frac{\partial^2 p}{\partial x^2}, \quad (\text{A.1})$$

in the semi-infinite line $x \geq 0$, with a semi-reflecting boundary in $x = 0$,

$$\left. \frac{\partial p}{\partial x} \right|_{x=0} = rp(x=0, t), \quad (\text{A.2})$$

and with initial condition $p(x, t=0) = \delta(x - x_0)$. We remind that within the PEP model, we have $r = 2\alpha$, see Eq. (9).

We define $q(x, t) = p'(x, t) - rp(x, t)$, where the prime indicates the derivative with respect to x , which still satisfies the diffusion equation (A.1), but with the easier boundary condition, $q(0, t) = 0$. The price to be paid is in the initial condition, $q(x, 0) = \delta'(x - x_0) - r\delta(x - x_0)$. The details of the calculation can be found in Ref. [30] and here we limit to write the solution

$$\begin{aligned} q(x, t) = & -\frac{1}{\sqrt{4\pi(Dt)^3}} \left[(x+x_0)e^{-\frac{(x+x_0)^2}{4Dt}} + (x-x_0)e^{-\frac{(x-x_0)^2}{4Dt}} \right] \\ & -\frac{r}{\sqrt{4\pi Dt}} \left[e^{-\frac{(x-x_0)^2}{4Dt}} - e^{-\frac{(x+x_0)^2}{4Dt}} \right] \end{aligned} \quad (\text{A.3})$$

and

$$p(x, t) = -\int_x^\infty q(s, t)e^{-r(s-x)} ds. \quad (\text{A.4})$$

What we need is the probability $F(t)$ that the particle is absorbed in $x = 0$ during the time interval $(t, t + dt)$, which is given by

$$F(t) = Dp'(0, t) = Drp(0, t) = -Dr \int_0^\infty q(x, t)e^{-rx} dx. \quad (\text{A.5})$$

Therefore, using (A.3) we obtain

$$\begin{aligned} F(t) = Dr \int_0^\infty dx e^{-rx} & \left\{ \frac{1}{\sqrt{4\pi(Dt)^3}} \left[(x+x_0)e^{-\frac{(x+x_0)^2}{4Dt}} + (x-x_0)e^{-\frac{(x-x_0)^2}{4Dt}} \right] \right. \\ & \left. + \frac{r}{\sqrt{4\pi Dt}} \left[e^{-\frac{(x-x_0)^2}{4Dt}} - e^{-\frac{(x+x_0)^2}{4Dt}} \right] \right\}. \end{aligned} \quad (\text{A.6})$$

We now formally evaluate the previous integral, which may be written in terms of the error function, $\text{erf}(x) = \frac{2}{\sqrt{\pi}} \int_0^x e^{-s^2} ds$. Then, we evaluate the limiting behaviors of $F(t)$, at short and long times. We need to calculate the following integrals,

$$I_1(x_0) = \int_0^\infty dx e^{-rx} e^{-\frac{(x+x_0)^2}{4Dt}} \quad (\text{A.7})$$

$$= e^{rx_0} \sqrt{\pi Dt} e^{r^2 Dt} \left[1 - \text{erf} \left(r\sqrt{Dt} + \frac{x_0}{2\sqrt{Dt}} \right) \right] \quad (\text{A.8})$$

$$= e^{rx_0} \sqrt{\pi Dt} J_1(x_0, r, t) \quad (\text{A.9})$$

where

$$J_1(x_0, r, t) \equiv e^{r^2 Dt} \left[1 - \text{erf} \left(r\sqrt{Dt} + \frac{x_0}{2\sqrt{Dt}} \right) \right] \quad (\text{A.10})$$

and

$$I_2(x_0) = \int_0^\infty dx e^{-rx} (x + x_0) e^{-\frac{(x+x_0)^2}{4Dt}} \quad (\text{A.11})$$

$$= -e^{rx_0} \sqrt{\pi Dt} \frac{\partial}{\partial r} J_1(x_0, r, t), \quad (\text{A.12})$$

so that

$$F(t) = -\frac{r}{2t} [e^{rx_0} \partial_r J_1(x_0, r, t) + e^{-rx_0} \partial_r J_1(-x_0, r, t)] \quad (\text{A.13})$$

$$+ \frac{Dr^2}{2} [e^{rx_0} J_1(x_0, r, t) - e^{-rx_0} J_1(-x_0, r, t)]. \quad (\text{A.14})$$

- Limit $x_0^2 \ll Dt \ll r^{-2}$

Using the limit $\text{erf}(x) \simeq \frac{2}{\sqrt{\pi}}x$ for $x \ll 1$, we can write

$$J_1(x_0, r, t) \simeq 1 - \frac{2}{\sqrt{\pi}} \left(r\sqrt{Dt} + \frac{x_0}{2\sqrt{Dt}} \right) \quad (\text{A.15})$$

$$\partial_r J_1(x_0, r, t) \simeq -\frac{2}{\sqrt{\pi}} \sqrt{Dt} \quad (\text{A.16})$$

and

$$F(t) \simeq \frac{2}{\sqrt{\pi}} \sqrt{D} \frac{r}{\sqrt{t}}. \quad (\text{A.17})$$

- Limit $t \gg r^{-2}$

Using the limit $\text{erf}(x) \simeq 1 - \frac{e^{-x^2}}{\sqrt{\pi}x}$ for $x \gg 1$, we can write

$$J_1(x_0, r, t) \simeq \frac{1}{r\sqrt{\pi Dt}} \quad (\text{A.18})$$

$$\partial_r J_1(x_0, r, t) \simeq -\frac{1}{r^2 \sqrt{\pi Dt}} \quad (\text{A.19})$$

and

$$F(t) \simeq \frac{1}{r\sqrt{\pi D}} t^{-3/2}. \quad (\text{A.20})$$

Using $r = 2\alpha$, from (A.17) and (A.20), we find Eqs. (10).

Appendix B. Relaxation of a breather on an empty background

- Limit $x_0^2 \ll t \ll \alpha^{-2}$

Recalling that

$$\int_0^\infty dt F(t) = 1, \quad (\text{B.1})$$

we rewrite Eq. (11) as

$$\langle \Delta h(t) \rangle = \alpha \int_0^t dt' (1 - p_1(t')) \left[1 - \int_0^{t'} dt'' F(t'') \right]. \quad (\text{B.2})$$

Now, since at short times

$$\int_0^{t'} dt'' F(t'') \ll D^{1/2} \simeq 1 \quad (\text{B.3})$$

and $p_1 \ll 1$, we obtain to the leading order

$$\langle \Delta h(t) \rangle = \alpha t. \quad (\text{B.4})$$

- Limit $t \gg \alpha^{-2}$

Let us introduce an intermediate timescale t_0 such that $\alpha^{-2} \ll t_0 \leq t$. Therefore, Eq. (11) is rewritten as

$$\langle \Delta h(t) \rangle = \alpha \left[\int_0^{t_0} dt' (1 - p_1(t')) \int_0^{t'} dt'' F(t'') + \int_{t_0}^t dt' (1 - p_1(t')) \int_0^{t'} dt'' F(t'') \right]. \quad (\text{B.5})$$

In the regime $t \gg \alpha^{-2}$, $F(t)$ can be approximated as in Eq. (10) and $p_1(t) \simeq 1/2$. Consequently, one can compute explicitly the second addend in the square brackets, that gives

$$\int_{t_0}^t dt' (1 - p_1(t')) \int_0^{t'} dt'' F(t'') = \frac{1}{2} \int_{t_0}^t dt' \int_0^{t'} dt'' \frac{1}{2\alpha\sqrt{\pi Dt''^3}} = \frac{1}{\alpha} \sqrt{\frac{t}{\pi D}}. \quad (\text{B.6})$$

Therefore, for $t \geq t_0$

$$\langle \Delta h(t) \rangle = K(t_0) + \sqrt{\frac{t}{\pi D}}, \quad (\text{B.7})$$

where $K(t_0)$ is a constant. Finally, for $D = 1/2$, we obtain Eq. (13).

Appendix C. Random walk with two semi-reflecting boundaries

We have two breathers in $i = 0, L$ and a random walk in between, moving according to the following rules: if the particle is in $i \neq 1, L - 1$, it hops to $i \pm 1$ with probability $1/2$; if $i = 1$ ($i = L - 1$), it hops to $i = 2$ ($i = L - 2$) with probability q and to $i = 0$ ($i = L$), therefore being absorbed, with probability $1 - q$. We define the probability $P(L)$ that a particle released in $i = 1$ attaches to the breather in $i = L$.

It is also useful to define a model where the left boundary condition is the same as before, but the right boundary condition is symmetric, i.e. the particle hops from $i = L - 1$ to $i = L - 2, L$ with probability $1/2$. For this model we define the probability $p(L)$ that a particle released in $i = 1$ reaches the site $i = L$ before reaching the site $i = 0$. With these notations, we can write

$$P(L) = p \left(\frac{L}{2} \right) \frac{1}{2}, \quad (\text{C.1})$$

because a particle arrived in $L/2$ has the same probability to attach to the left or to the right breather. We now want to determine $p(L)$, summing up all the possible trajectories to go from $i = 1$ to $i = L$, without being absorbed in $i = 0$, according to the number n of passages in $i = 1$ (with $n \geq 1$). If a trajectory is characterized by a given n , it means that the particle has hopped from 1 to 2 (which happens with probability q) and $(n - 1)$ times it has come back to 1 before attaining L (which occurs with probability $(1 - a)$, with $a = 1/L$), and one time has attained L before coming back to 1 (which occurs with probability a). Summing up all terms, we have

$$p(L) = \sum_{n \geq 1} q^n (1 - a)^{n-1} a \quad (\text{C.2})$$

$$= \frac{a}{1 - a} \sum_n q^n (1 - a)^n \quad (\text{C.3})$$

$$= \frac{aq}{(1 - q) + qa}, \quad (\text{C.4})$$

with $a = 1/L$. So, we get

$$P(L) = p \left(\frac{L}{2} \right) \frac{1}{2} \quad (\text{C.5})$$

$$= \frac{q}{2q + L(1 - q)} \quad (\text{C.6})$$

$$= \frac{1}{2 + L(q^{-1} - 1)}. \quad (\text{C.7})$$

Let us now define q in the most general way. If a particle is in $i = 1$, it has a probability $1/4$ to move to the right and a probability $\alpha/2$ to move to the left,⁺ so

$$q = \frac{\frac{1}{4}}{\frac{1}{4} + \frac{\alpha}{2}} = \frac{1}{1 + 2\alpha}, \quad (\text{C.8})$$

and

$$P(L) = \frac{1}{2} \frac{1}{1 + L\alpha}. \quad (\text{C.9})$$

References

- [1] Eilbeck J, Lomdahl P and Scott A 1985 Physica D **16** 318–338
- [2] Kevrekidis P G 2009 The Discrete Nonlinear Schrödinger Equation (Springer Verlag, Berlin)
- [3] Holstein T 1959 Annals of Physics **8** 325–389
- [4] Tsironis G and Hennig D 1999 Phys. Rep. **307** 333–432
- [5] Trombettoni A and Smerzi A 2001 Physical Review Letters **86** 2353
- [6] Hennig H, Neff T and Fleischmann R 2016 Physical Review E **93** 032219
- [7] Franzosi R, Livi R, Oppo G and Politi A 2011 Nonlinearity **24** R89
- [8] Jensen S 1982 Quantum Electronics, IEEE Journal of **18** 1580–1583
- [9] Christodoulides D and Joseph R 1988 Optics letters **13** 794–796
- [10] Rumpf B and Newell A C 2001 Physical Review Letters **87** 054102
- [11] Borlenghi S, Wang W, Fangohr H, Bergqvist L and Delin A 2014 Physical review letters **112** 047203
- [12] Borlenghi S, Iubini S, Lepri S, Chico J, Bergqvist L, Delin A and Fransson J 2015 Physical Review E **92** 012116
- [13] Scott A 2003 Nonlinear science. Emergence and dynamics of coherent structures (Oxford University Press, Oxford)
- [14] Rasmussen K, Cretegny T, Kevrekidis P and Grønbech-Jensen N 2000 Phys. Rev. Lett. **84** 3740–3743
- [15] Johansson M and Rasmussen K Ø 2004 Physical Review E **70** 066610
- [16] Flach S and Gorbach A V 2008 Physics Reports **467** 1–116
- [17] Iubini S, Franzosi R, Livi R, Oppo G L and Politi A 2013 New Journal of Physics **15** 023032
- [18] Rumpf B 2004 Phys. Rev. E **69** 016618
- [19] Rumpf B 2007 EPL (Europhysics Letters) **78** 26001
- [20] Rumpf B 2008 Physical Review E **77** 036606
- [21] Rumpf B 2009 Physica D: Nonlinear Phenomena **238** 2067–2077
- [22] Iubini S, Politi A and Politi P 2014 Journal of Statistical Physics **154** 1057–1073
- [23] Kuramoto Y 2012 Chemical oscillations, waves, and turbulence vol 19 (Springer Science & Business Media)
- [24] Krapivsky P L, Redner S and Ben-Naim E 2010 A kinetic view of statistical physics (Cambridge University Press)
- [25] Edwards S F and Wilkinson D 1982 The surface statistics of a granular aggregate Proceedings of the Royal Society of London A: Mathematical, Physical and Engineering Sciences vol 381 (The Royal Society) pp 17–31
- [26] Basile G, Bernardin C and Olla S 2006 Phys. Rev. Lett. **96** 204303
- [27] Lepri S, Mejía-Monasterio C and Politi A 2009 J. Phys. A: Math. Theor. **42** 025001

⁺ Each probability is the product of $1/2$ (the probability to choose right or left) with the probability to actually make the move.

- [28] Lepri S, Mejía-Monasterio C and Politi A 2010 Journal of Physics A: Mathematical and Theoretical **43** 065002
- [29] Delfini L, Lepri S, Livi R, Meja-Monasterio C and Politi A 2010 J. Phys. A: Math. Theor. **43** 145001
- [30] Weiss G H 1994 Aspects and applications of the random walk (Amsterdam: North-Holland)